ACS Partner Journal

Journal of the American Society for Mass Spectrometry

pubs.acs.org/jasms

Research Article

Post-Column Denaturation-Assisted Native Size-Exclusion Chromatography–Mass Spectrometry for Rapid and In-Depth Characterization of High Molecular Weight Variants in Therapeutic Monoclonal Antibodies

Yuetian Yan,* Tao Xing, Anita P. Liu, Zhengqi Zhang, Shunhai Wang,* and Ning Li

Cite This: *J. Am. Soc. Mass Spectrom.* 2021, 32, 2885–2894

Read Online

ACCESS | Metrics & More | Article Recommendations | Supporting Information

ABSTRACT: The high molecular weight (HMW) size variants present in therapeutic monoclonal antibody (mAb) samples need to be closely monitored and characterized due to their impact on product safety and efficacy. Because of the complexity and often low abundances in final drug substance (DS) samples, characterization of such HMW species is challenging and traditionally requires offline enrichment of the HMW species followed by analysis using various analytical tools. Here, we report the development of a postcolumn denaturation-assisted native SEC-MS method that allows rapid and in-depth characterization of mAb HMW species directly from unfractionated DS samples. This method not only provides high-confidence identification of HMW complexes based on accurate mass measurement of both the intact assembly and the constituent subunits but also allows in-depth analysis of the interaction nature and location. In addition, using the extracted ion chromatograms, derived from high-quality, native-like mass spectra, the elution profiles of each noncovalent and/or nondissociable complex can be readily reconstructed, facilitating the comprehension of a complex HMW profile. The utility of this novel method was demonstrated in different applications, ranging from enriched HMW characterization at late stage development, comparability assessment due to process changes, and forced degradation study of coformulated mAbs. As this method does not require prior enrichment, it is thus desirable for providing both rapid and in-depth characterization of HMW species during the development of therapeutic mAbs.

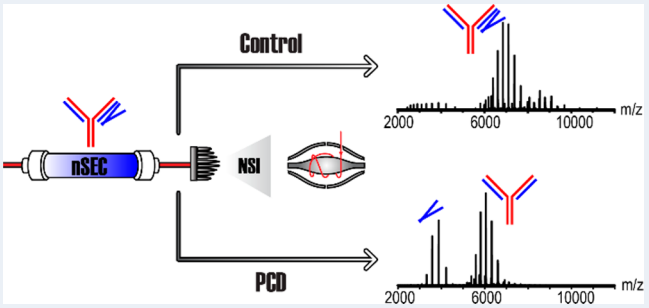

INTRODUCTION

Therapeutic monoclonal antibodies (mAbs) often exhibit some degree of size heterogeneity containing product-related impurities, including high molecular weight (HMW) aggregates and low molecular weight (LMW) fragments. These species often arise from physical, chemical and enzymatic degradation of the mAb molecules due to environmental stresses during product manufacture, shipping, and storage.[1−3] LMW fragments can be generated via different chemical or enzymatic degradation pathways (e.g., acid-, base- and enzyme-driven hydrolysis of polypeptide bonds, interchain disulfide bond breakage, and so forth), yielding truncated forms of the mAb molecule.[4,5] In contrast, the formation of mAb HMW species is a much more complex process. The generated HMW forms can vary in size, conformation, interaction nature (covalent or noncovalent), and site of association.[6] Besides the stress conditions, the antibody primary sequence, as well as its higher-order structure, all contribute to its tendency to aggregation via different pathways. Therefore, it is nearly impossible to use a general rule to predict or describe the mAb aggregation behavior of each molecule. As mAb HMW species (from soluble oligomers to visible particles) may impact drug safety and efficacy by eliciting unwanted immunogenic responses and/or altering its pharmacokinetic behaviors,[7] detailed characterization, continuous monitoring, and control of the HMW species throughout the product life cycle are required.[8] In addition, deep understanding of the mAb aggregation mechanisms, as achieved by in-depth characterization, not only provides the framework for risk assessment of HMW species but might also offer insight for designing mAb molecules with reduced aggregation propensity through protein engineering.

Characterization of HMW size variants in mAb products often relies on an arsenal of analytical and biophysical tools due to their complexity. Both sedimentation velocity analytical

Received: September 16, 2021
Revised: November 1, 2021
Accepted: November 2, 2021
Published: November 17, 2021

ultracentrifugation (SV-AUC)[9,10] and size exclusion chromatography (SEC) have been widely used in characterizing mAb HMW species due to their excellent resolving power and quantitative performance. In particular, SEC with UV detection is routinely used as a batch release assay to directly monitor the level and elution profile of soluble aggregates in therapeutic mAb products.[11,12] To enable detailed elucidation of the HMW species and gain insights on aggregation mechanisms, enrichment of the mAb HMW species followed by in-depth characterization by other techniques is almost always required.[6,13−17] For example, capillary electrophoresis-sodium dodecyl sulfate (CE-SDS) performed under nonreducing conditions can be used to differentiate and estimate the levels of covalently and noncovalently bound HMW species.[13,15,17] Moreover, when operated under reducing conditions, CE-SDS can further evaluate the possible contribution from intermolecular disulfide bond scrambling to the formation of covalent aggregates. Limited enzymatic digestion (e.g., IdeS digestion and limited Lys-C digestion) followed by mass spectrometry (MS) analysis has also proven effective in determining the aggregation interfaces at subdomain levels based on accurate mass measurement.[13,15−17] Finally, to achieve peptide-level or even residue-level elucidation of the aggregation interfaces and mechanisms, more sophisticated strategies, such as protein footprinting (e.g., hydrogen−deuterium exchange MS[18−20] and hydroxyl radical footprinting[21]) and bottom-up-based cross-linking analyses, can be applied to study the noncovalent and covalent HMW species, respectively.

Over the past decade, online coupling of SEC with direct MS detection has evolved from its initial application under denaturing conditions[22] to under near native conditions (native SEC-MS)[23] and has gained a lot of interest in studying mAb HMW species.[13,24,25] Using MS-compatible mobile phases that can preserve protein conformation and noncovalent interactions, native SEC-MS (nSEC-MS) can provide rapid and improved identification of mAb size variants based on accurate mass measurement. In addition, thanks to the recent advances in both methodology and instrumentation, nSEC-MS has become a highly sensitive method that can readily detect very low levels of HMW species (e.g., at 0.1%) directly from unfractionated drug substance (DS) samples.[26] Despite these notable successes, application of the nSEC-MS method alone still cannot obtain a complete picture of the mAb HMW profile. First, as a nondenaturing method nSEC-MS analysis does not distinguish between the noncovalently and covalently bound HMW complexes, unless clear mass differences resulting from the covalent cross-links can be detected. Unfortunately, the latter can be extremely difficult to achieve, due to both insufficient chromatographical resolution and mass resolving power for large mAb complexes. For instance, mAb dimer species formed by different mechanisms (e.g., noncovalent and covalent interactions) are often coeluting during SEC separation and measured with an averaged mass by MS detection. Therefore, the distribution of noncovalent and covalent dimer species cannot be directly determined by nSEC-MS method. Second, compared to well-expected oligomeric species (e.g., dimer, trimer, tetramer, and so forth), confident identification of unconventional HMW species (e.g., mAb monomer complexed with additional light chains[14,20]) often cannot be established by intact mass measurement alone. This is because reduced mass accuracy is often expected for mass measurement of large HMW species present at low abundances, which can lead to ambiguous mass assignments.

To overcome these challenges, we describe a new postcolumn denaturation-assisted nSEC-MS method (PCD-assisted nSEC-MS) that is optimized to dissociate SEC-resolved, noncovalent mAb HMW species into constituent components for subsequent MS detection. As a result, this new approach enables simultaneous detection of both noncovalent and nondissociable (covalent or tightly associated noncovalent) HMW species under identical SEC separation conditions. In addition, this strategy improves the identification of heterogeneous HMW species by (1) confirming the identities of the constituent subunits dissociated from the noncovalent HMW complexes; and (2) achieving more accurate mass measurement of nondissociable HMW species by removing interference from coeluting, noncovalent species. Furthermore, by incorporating a limited enzymatic digestion step, the PCD-assisted nSEC-MS method can readily reveal both the interaction nature and interaction interfaces of mAb aggregates at subdomain levels. Finally, the utility of this method is demonstrated in different case studies, ranging from enriched HMW characterization at late stage development, comparability assessment due to process changes, and forced degradation study of coformulated mAbs. We demonstrate this PCD-assisted nSEC-MS method as a powerful tool in performing rapid and in-depth characterization of mAb HMW species not only from enriched HMW samples but also from unfractionated DS samples, where HMW species are present at low levels.

EXPERIMENTAL SECTION

Materials. Deionized water was provided by a Milli-Q integral water purification system installed with a MilliPak Express 20 filter (Millipore Sigma, Burlington, MA). Ammonium acetate (LC/MS grade) was purchased from Sigma-Aldrich (St. Louis, MO). Peptide N-glycosidase F (PNGase F) was purchased from New England Biolabs Inc. (Ipswich, MA). FabRICATOR was purchased from Genovis (Cambridge, MA). Invitrogen UltraPure 1 M Tris-HCl buffer, pH 7.5, Pierce DTT (dithiothreitol, No-Weigh Format), and acetonitrile (ACN; Optima LC/MS grade) were obtained from Thermo Fisher Scientific (Waltham, MA). Formic acid (FA, 98−100%, Suprapur for trace metal analysis) was purchased from Millipore Sigma (Burlington, MA). 2-Propanol (IPA; HPLC grade) was purchased from Sigma-Aldrich (St. Louis, MO).

Sample Preparation. All mAbs were produced in CHO cells at Regeneron Pharmaceuticals, Inc. The mAb3 enriched HMW sample was generated by fractionating the HMW species from a mAb3 DS sample using a semipreparation scale SEC column. The final enriched HMW sample contains 0.7% trimer, 66.8% dimer, and 32.5% monomer. Prior to desalting SEC-MS analysis, limited reduction was performed by treating mAb1 with 2 mM DTT in 50 mM Tris-HCl (pH 7.5) at 37 °C for 30 min to only reduce interchain disulfide bonds. For intact level analysis, all mAb samples, including enriched HMW samples, individual DS samples, and coformulated DP samples, were treated with PNGase F (1 IUB milliunit per 10 μg of protein) at 45 °C in 50 mM Tris-HCl (pH 7.0) for 1 h to remove the N-glycan chains from each heavy chain CH2 domain. For subdomain analysis, an aliquot of the deglycosylated mAb3 HMW sample and mAb4 DS samples was each subjected to site-specific digestion with FabRICATOR (1 IUB

https://doi.org/10.1021/jasms.1c00289
J. Am. Soc. Mass Spectrom. 2021, 32, 2885−2894

milliunit per 1 μg of protein) in 50 mM Tris-HCl (pH 7.5) at 37 °C for 1 h, to generate the $F(ab)'_2$ and Fc fragments.

PCD-Assisted nSEC-MS. Native SEC chromatography was performed on an UltiMate 3000 UHPLC System (Thermo Fisher Scientific, Bremen, Germany) equipped with an Acquity BEH200 SEC column (4.6 × 300 mm, 1.7 μm, 200 Å; Waters, Milford, MA) with the column compartment set to 30 °C. An isocratic flow of 150 mM ammonium acetate at 0.2 mL/min was applied to separate and elute protein size variants. To enable postcolumn denaturation, a denaturing solution consisting of 60% ACN, 36% water, and 4% FA was delivered by a secondary pump at a flow rate of 0.2 mL/min and then mixed with the SEC eluent (1:1 mixing) using a T-mixer before being subjected to MS detection. To enable online native MS analysis, the combined analytical flow (0.4 mL/min) was split into a microflow (<10 μL/min) for nanoelectrospray ionization (NSI)-MS detection and a remaining high flow for UV detection (Figure 1,). A Thermo Q Exactive UHMR

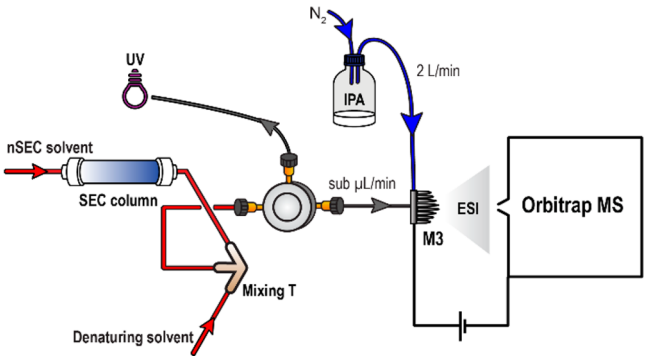

Figure 1. Scheme of a PCD-assisted nSEC-MS platform

(Thermo Fisher Scientific, Bremen, Germany) equipped with a microflow-nanospray electrospray ionization (MnESI) source and a microfabricated monolithic multinozzle (M3) emitter (Newomics, Berkley, CA) was used for native MS analysis. A detailed experimental setup and instrument parameters can be found in a previous publication.[26] To disable PCD, the flow of the denaturing solution was set to zero. Desalting SEC-MS analysis of the partially reduced mAb1 was performed in a similar fashion using an Acquity BEH200 SEC guard column (4.6 × 30 mm, 1.7 μm, 200 Å).

Data Analysis. Intact mass spectra from nSEC-MS analysis under native or PCD conditions were deconvoluted using Intact Mass software from Protein Metrics (Cupertino, CA).

RESULTS AND DISCUSSION

A PCD-Assisted nSEC-MS Method. To improve nSEC-MS-based characterization of mAb HMW species, a post-column denaturation (PCD) strategy is introduced to dissociate noncovalent HMW complexes after SEC separation before MS detection. This strategy is highly desirable as it not only enables improved assignment of noncovalent HMW complexes by confirming the constituent subunits but also provides more accurate mass measurement of nondissociable HMW species by reducing the interference from coeluting, noncovalent species. Taking advantage of a previously described nLC-MS platform that can accommodate a high flow rate (up to 0.8 mL/min), integration of PCD with nSEC-MS can be readily achieved by introducing a postcolumn denaturant flow (0.2 mL/min) to the nSEC flow (0.2 mL/min) via a T-mixer (Figure 1). The denaturing solvent was carefully selected based on two primary considerations. First, the final flow after postcolumn mixing should still be highly compatible with direct MS detection. Second, because of the short denaturation time (e.g., less than 1 s from the T-mixer to MS), the desired denaturing solvent should be capable of disrupting the majority of the noncovalent interactions instantaneously after postcolumn mixing.

After evaluating a series of denaturing solvent systems containing varying levels of acetonitrile (ACN) and formic acid (FA), an optimized formula comprised of 60% ACN, 4% FA, and 36% water was selected for PCD application. To assess the effectiveness of the selected denaturing solvent, mAb1 (IgG4 subclass) was partially reduced (interchain disulfide bonds disrupted) and subjected to PCD-assisted nSEC-MS analysis using a short SEC guard column (Figure 2a). Because of the

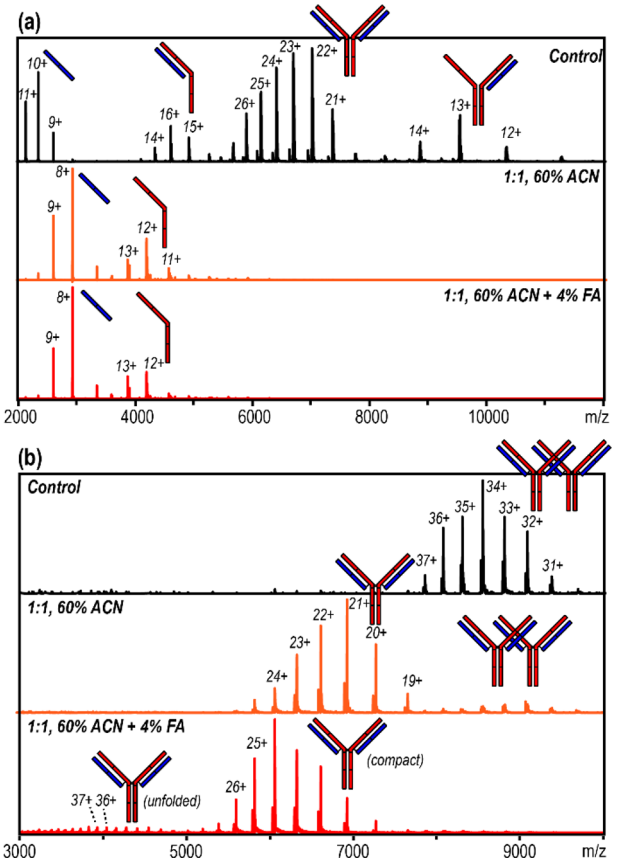

Figure 2. (a) Mass spectra of partially reduced mAb1 (interchain disulfide bonds disrupted) obtained under native (black trace) or PCD conditions (orange and red traces). (b) Mass spectra of mAb2 dimer obtained under native (black trace) or PCD (orange and red traces) conditions.

strong interchain noncovalent interactions between the two CH3 domains and between the N-terminal regions of heavy and light chains (HC and LC) in IgG4 molecules,[27] the partially reduced mAb1 was predominantly detected as an intact H2L2 complex under nSEC-MS conditions. Only low levels of HL, H2L, and LC species were observed, which were likely generated via in-source dissociation (Figure 2a, black trace). In contrast, after applying PCD conditions (60% ACN/4% FA), these noncovalent complexes (e.g., H2L2, H2L, and HL) were completely dissociated and detected as free HC and

https://doi.org/10.1021/jasms.1c00289
J. Am. Soc. Mass Spectrom. 2021, 32, 2885−2894

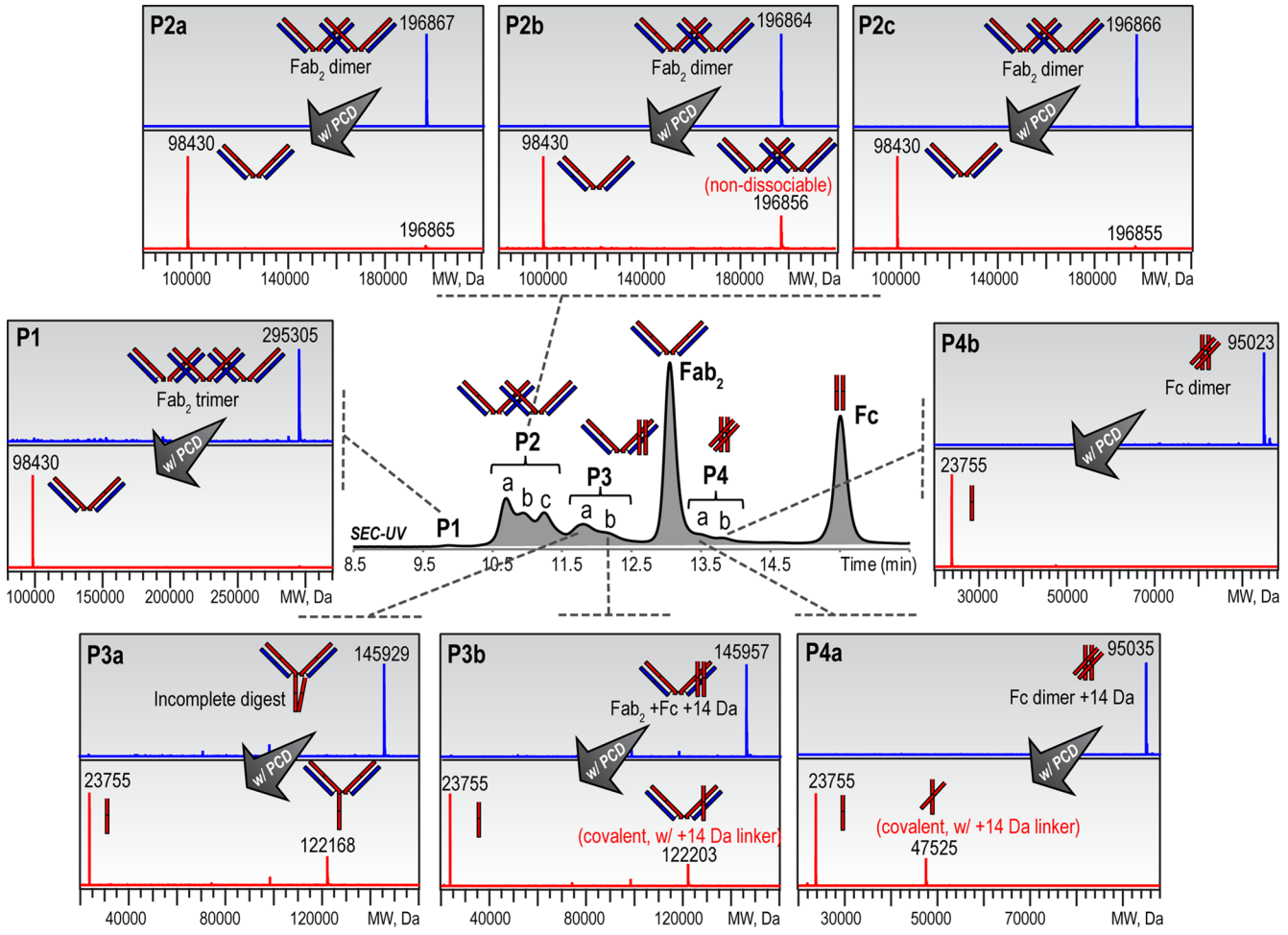

Figure 3. nSEC-UV/MS analysis of mAb3 enriched HMW sample after IdeS digestion displaying the SEC-UV trace (central panel), peak assignment, and the deconvoluted mass spectra for each HMW peak obtained under native (blue traces) or PCD (red traces) conditions.

LC (Figure 2a, red trace). An alternative denaturing solvent containing only 60% ACN was also tested, which showed comparable effectiveness in dissociating the partially reduced mAb complex (Figure 2a, orange trace). In another example, the mAb2 dimer species detected by nSEC-MS analysis (Figure 2b, black trace) displayed a near-complete dissociation into monomers upon application of PCD (60% ACN/4% FA) (Figure 2b, red trace), suggesting the majority, if not all, of the dimer species were noncovalent. In addition, low levels of highly charged monomer signal, corresponding to the unfolded species, were also observed in the low m/z region. Unlike the first example, application of the alternative denaturing solvent containing 60% ACN alone did not lead to a complete dissociation of the mAb2 dimer species (Figure 2b, orange trace), suggesting the combination of low pH and organic solvent is more effective in disrupting the noncovalent interactions. Subsequently, the developed PCD conditions have also been applied to other noncovalent systems (e.g., antibody−antigen complexes and virus capsids), where rapid and effective dissociation could always be achieved (data not shown). Therefore, the developed PCD conditions are considered effective in disrupting the majority of noncovalent interactions present in mAb HMW complexes, although it is still possible that some tightly associated noncovalent complexes may survive the treatment. Lastly, it is important to note that by applying the reported nLC-MS platform,[26] the mAb-related species all exhibited "native-like" mass spectra under the selected PCD conditions (60% ACN/4% FA), which exhibited low charge density, narrow charge state distributions, and distinct m/z region for ionic peak clusters representing protein/fragment species of different sizes.[28] This feature is highly desirable, as it reduces the spectral crowding from multiple species that are simultaneously dissociated from the same complexes and detected in the same MS scan. For example, under PCD conditions, the MS signal of the dissociated HC and LC were well isolated on the m/z scale with minimal overlapping (Figure 2a). In addition, compared to typical ESI-MS spectra under denaturing conditions, "native-like" spectra exhibit much fewer charge states and greater spatial resolution, making them easier to be interpreted and processed (e.g., generating extracted ion chromatograms).

PCD-Assisted nSEC-MS Analysis of Enriched HMW Species. Extended characterization of mAb HMW species is often required at the late stage of program development, as part of the DS heterogeneity characterization. Limited enzymatic digestion (e.g., IdeS digestion) followed by intact mass analysis is frequently performed on the enriched HMW material to understand the interaction interfaces at subdomain levels. For this purpose, a mAb3 enriched HMW sample mainly containing dimeric species was treated with IdeS digestion before subjected to PCD-assisted nSEC-MS analysis. As IdeS cleaves the mAb molecule under the hinge region

https://doi.org/10.1021/jasms.1c00289
J. Am. Soc. Mass Spectrom. 2021, 32, 2885−2894

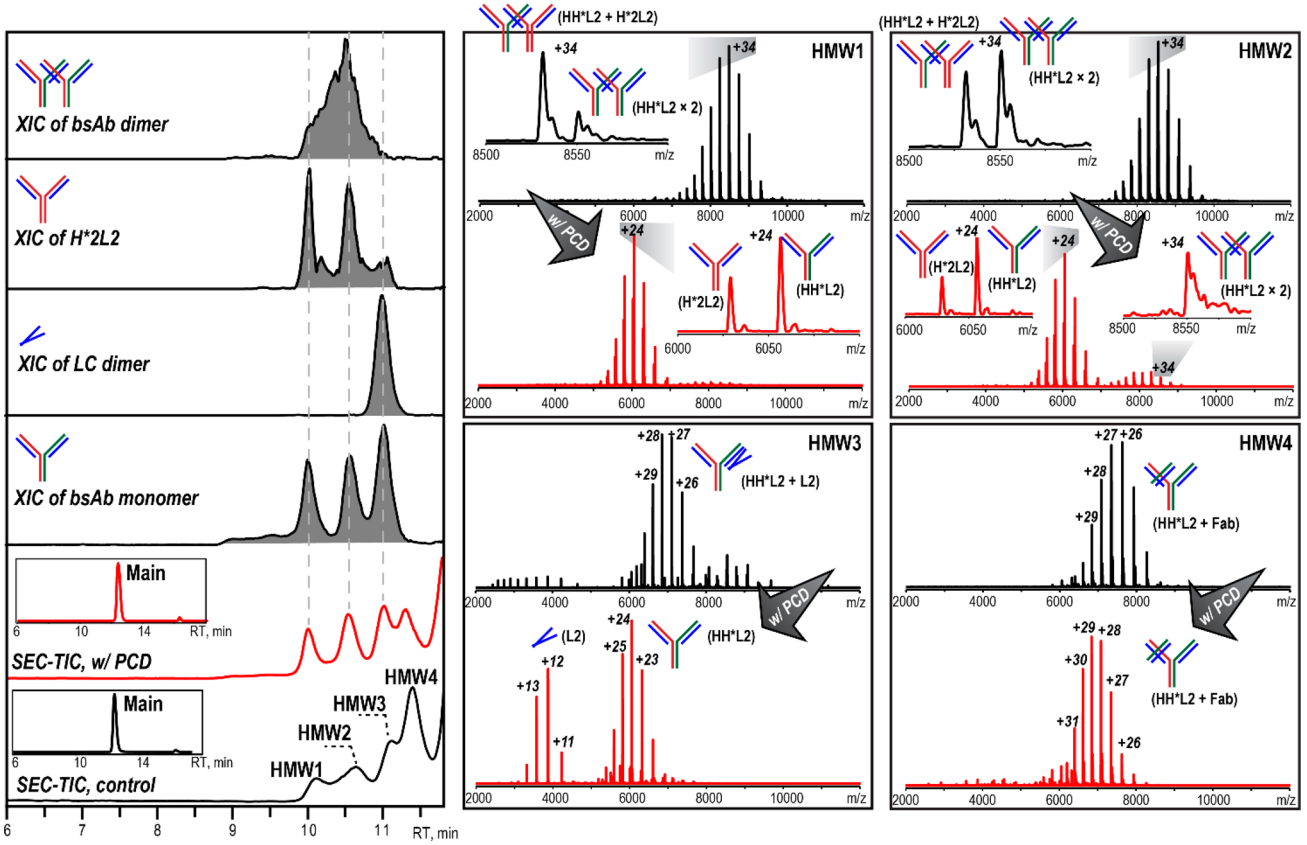

Figure 4. nSEC-UV/MS analysis of bsAb DS sample displaying the SEC-TICs (left panel, red and black traces) and the raw mass spectra for each HMW peak obtained under native (black traces) or PCD (red traces) conditions. The XICs were generated using the most abundant charge state of each species (gray traces, left panels).

releasing F(ab)′$_2$ and Fc fragments, this strategy allows effective characterization of the dimeric interactions at subdomain levels. SEC-UV analysis of the digested HMW sample (Figure 3, middle) exhibited multiple resolved UV peaks, including two major ones corresponding to F(ab)′$_2$ and Fc monomers, and four other peaks (P1−P4) likely corresponding to HMW-related species as a result of various subdomain interactions present in the enriched HMW sample. Subsequently, the accurate mass measurement from nSEC-MS analysis was used to assign the identity of each peak (Figure 3, Table S1). Although intact mass measurement of the native complexes can readily differentiate aggregation states and interacting partners (e.g., F(ab)′$_2$ trimer in P1, F(ab)′$_2$ dimer in P2, F(ab)′$_2$-Fc heterodimer in P3, and Fc dimer in P4), detailed elucidation of each species was still challenging due to a considerable amount of ambiguity from intact mass-based assignments. For example, the Fc dimer in P4b exhibited an observed mass (95 023 Da) consistent with the predicted mass of a noncovalent dimer (95 018 Da), while the Fc dimer in P4a exhibited a mass increase of approximately 14 Da (Figure 3) compared to the predicted mass. This mass increase can be potentially attributed to the presence of either an oxidation modification (+16 Da) within a noncovalent complex or a covalent cross-link (e.g., 14 Da between two histidine residues) maintaining a covalent complex. Unfortunately, the mass resolution and accuracy achieved at the intact complex level cannot lead to an unambiguous assignment and differentiate the two very different scenarios. Similarly, confident elucidation of F(ab)′$_2$-Fc heterodimer in P3 was also compounded by the possible coexistence of both noncovalent and covalent dimer species, as well as incomplete reaction products from IdeS digestion, all of which would only exhibit small mass differences between each other. Finally, although nSEC-MS analysis readily confirmed that the three partially resolved peaks, P2a, P2b, and P2c, all contained F(ab)′$_2$ dimer species with similar observed masses (196 864−196 867 Da), no other meaningful information can be retrieved from this analysis to characterize the apparently heterogeneous F(ab)′$_2$−F(ab)′$_2$ interactions present in the HMW sample.

To reduce the ambiguities and improve the characterization, PCD was implemented post-SEC separation to provide a second dimension of separation based on interaction nature. For example, under PCD conditions distinctive dissociation behaviors were observed for the Fc dimer species in P4a and P4b. The Fc dimer in P4b, which had already been tentatively assigned as a noncovalent species based on the observed mass of the native complex, underwent a complete dissociation into Fc/2 subunits under PCD conditions. This result confirmed the noncovalent nature of the Fc dimer in P4b. In contrast, application of PCD in P4a led to the formation of both Fc/2 subunits (e.g., dissociated from the noncovalent Fc complex) and a nondissociable Fc/2 dimer species. Consistent with the larger mass of the Fc dimer in P4a as detected under native conditions, the nondissociable Fc/2 dimer also showed a mass increase of approximately 14 Da compared to that of a noncovalent Fc/2 dimer. This delta mass was proposed to correspond to a previously reported covalent cross-link that occurs between two histidine (His) residues (cross-linker mass: 13.98 Da).[29−31] Subsequent peptide mapping analysis also identified several His−His cross-linked dipeptides from

https://doi.org/10.1021/jasms.1c00289
J. Am. Soc. Mass Spectrom. 2021, 32, 2885−2894

the Fc region that likely contributed to the Fc dimer in P4a (data not shown). The same covalent cross-link was also observed for the $F(ab)'_2$-Fc dimer in P3b, which was measured ~14 Da higher in mass comparing to that of a noncovalent $F(ab)'_2$−Fc dimer. Application of PCD further confirmed this assignment by dissociating this species into a Fc/2 subunit and a nondissociable $F(ab)'_2$−Fc/2 complex that also exhibited a mass increase of approximately 14 Da due to the His−His cross-link. In contrast, the species in P3a displayed an observed mass approximately 18 Da lower than that of a noncovalent $F(ab)'_2$−Fc dimer and was readily dissociated into an Fc/2 and a complementary Fc/2-clipped mAb species under PCD conditions. Therefore, the species in P3a was assigned as an incomplete IdeS digestion product with only one heavy chain cleaved. Finally, despite the similar observed masses at the intact complex level, the $F(ab)'_2$ dimer in P2b exhibited different dissociation behavior than those in P2a and P2c under PCD conditions (Figure 3). Specifically, with PCD applied the dimer species in P2a and P2c underwent a near-complete dissociation, leading to the detection of solely $F(ab)'_2$ monomers. This observation indicated the non-covalent nature of the $F(ab)'_2$ dimers in both P2a and P2c, which were separated by SEC likely due to conformational differences. In contrast, P2b showed a significant amount of $F(ab)'_2$ dimer remained nondissociable under PCD conditions, suggesting the presence of a "covalent-like" $F(ab)'_2$ dimer. Additionally, as the coeluting, noncovalent $F(ab)'_2$ dimer was dissociated, a more accurate mass measurement of the nondissociable dimer in P2b could be achieved. Indeed, this analysis revealed that the nondissociable dimer in P2b exhibited a lower mass (196 856 Da) than that of a noncovalent dimer (theoretical mass: 196 866 Da), suggesting the possible presence of a covalent cross-link with a negative delta mass. Although identification of this covalent cross-link is still ongoing and outside the scope of this manuscript, the information from the PCD-assisted nSEC-MS analysis is valuable to guide the investigation.

PCD-Assisted nSEC-MS Analysis of HMW Species in Unfractionated DS Samples. Direct analysis of HMW species from unfractionated mAb DS samples is highly desirable, as it is less resource-demanding and eliminates potential changes in the HMW profile (e.g., artificial HMW formation or dissociation of labile HMW species) due to sample handling. To demonstrate the applicability of the PCD-assisted nSEC-MS method in elucidating complex HMW species from unfractionated samples, a bispecific antibody (bsAb) DS sample, which exhibited a complicated HMW profile (four partially resolved HMW peaks) during SEC separation, was subjected to the analysis (Figure 4). Consisting of two identical light chains (LC) and two different heavy chains (HC and HC*), the bsAb (HH*L2) DS samples often contain low levels of monospecific mAb impurities (H2L2 and H*2L2) that can further contribute to the increased complexity of the HMW species. For example, nSEC-MS analysis indicated the presence of two different dimers in both HMW1 and HMW2 peaks, including a bsAb homodimer (HH*L2 × 2) and a heterodimer (HH*L2 + H*2L2) consisting of a bsAb and a monospecific H*2L2 species (deconvoluted mass shown in Table S2). The relative abundance of the heterodimer species is slightly higher in HMW1 peak compared to HMW2 peak. The application of PCD further supported these assignments, where both bsAb and H*2L2 monomers were dissociated from the dimer species and detected in HMW1 and HMW2 peaks. Interestingly, the application of PCD resulted in a complete dissociation of the heterodimers in both HMW1 and HMW2 peaks, indicating the noncovalent nature of these species. In contrast, the bsAb homodimers in HMW2 peak underwent a partial dissociation while a noticeable amount remained intact under PCD conditions, suggesting the presence of the nondissociable bsAb homodimer. As the monomer species can only be generated from the dissociation of the noncovalent dimers under PCD conditions, the extracted ion chromatograms (XICs) constructed using the monomer signal (e.g., bsAb monomer and H*2L2 monomer) could represent the elution profiles of the noncovalent dimers. Meanwhile, the XIC constructed using the bsAb homodimer signal under PCD conditions could represent the elution profile of the nondissociable bsAb homodimers. Applying this strategy, it was clear that both the noncovalent homodimer and the noncovalent heterodimer eluted in HMW1 and HMW2 peaks, while the nondissociable bsAb homodimer eluted in a broad and distinctive region with the peak apex aligned with HMW2 peak (Figure 4, left panel). Similarly, based on accurate mass measurement, the nSEC-MS analysis tentatively identified the HMW3 peak as a complex comprised of a bsAb monomer and two extra LCs. Subsequently, application of PCD not only confirmed the proposed composition but also revealed that the two extra LCs were present as a non-dissociable dimer (e.g., likely via interchain disulfide bond) and then associated with a bsAb molecule via noncovalent interactions. The XICs of the dissociated LC dimer and the bsAb monomer also confirmed their coelution with HMW3 peak, further supporting this assignment. Lastly, based on accurate mass measurement, the species in HMW4 peak was proposed to be a complex consisting of a bsAb monomer and a Fab fragment due to a clipping in CH_2 domain. As this species remained intact under PCD conditions, we think that it was a degradation product resulting from the truncation of the nondissociable bsAb homodimer species.

The ability to elucidate the HMW species directly from unfractionated DS samples makes the PCD-assisted nSEC-MS method ideally suited for process development support, where fast turn-around is desired to facilitate decision-making. To test the utility in this area, the method was then applied to assess the comparability of the HMW profile of the mAb program before and after process changes. As demonstrated in the SEC-UV traces, the HMW profiles of mAb4 DS lots before and after the process changes were generally comparable with minor differences in peak shape (Figure 5a, black trace). With accurate mass measurement from the nSEC-MS analysis, the predominant HMW peaks in both lot 1 and lot 2 were readily identified as mAb4 dimer species (Figure 5a, black trace). Application of PCD then revealed the presence of both the noncovalent dimer (Figure 5a, magenta trace, represented by the XIC of mAb4 monomer signal under PCD conditions) and the nondissociable dimer (Figure 5a, blue trace, represented by the XIC of nondissociated mAb4 dimer signal under PCD conditions) in both DS lots. It is clear that, although the HMW species were considered generally comparable based on UV peaks and the observed masses, the distributions of the noncovalent dimer and the nondissociable dimer were largely different between the two lots. Specifically, lot 2 contained a significantly higher level of the noncovalent dimer species, while lot 1 contained a notably higher level of the nondissociable dimer species. Moreover, the relative abundance of the noncovalent dimer within the total HMW species

https://doi.org/10.1021/jasms.1c00289
J. Am. Soc. Mass Spectrom. 2021, 32, 2885−2894

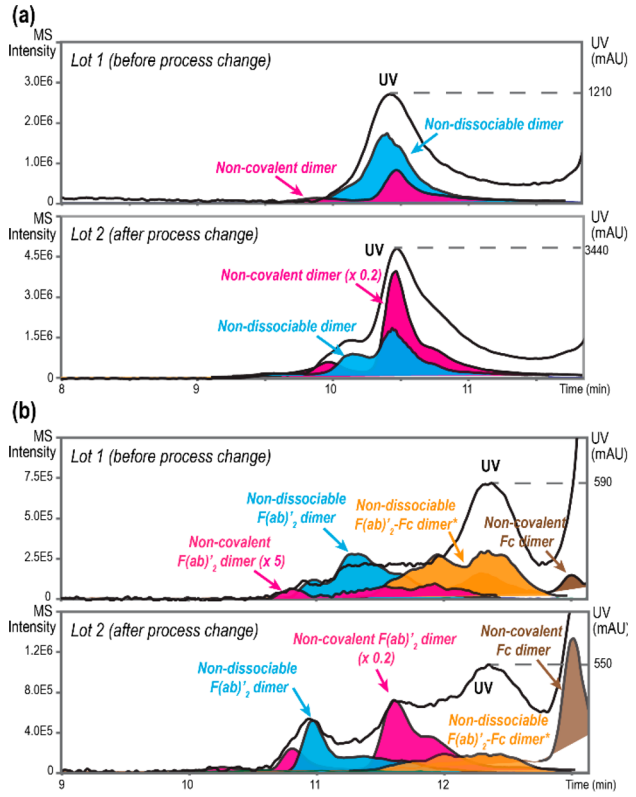

Figure 5. HMW profiles of mAb4 DS lot 1 and lot 2 characterized at (a) intact level and (b) subdomain level (after IdeS digestion) using PCD-assisted nSEC-UV/MS analysis. The UV profile (black trace) and XICs (colored traces) representing the elution profile of each HMW-related species are shown (only HMW region displayed). The XICs were generated using the most abundant charge state of each species.

can also be estimated based on the UV peak areas and the XICs generated from the PCD-assisted nSEC-UV/MS analysis using the following equation

$$\frac{\text{Noncovalent dimer}}{\text{Total dimer}}\% = \frac{\text{XIC}_{\text{Dimer}}/\text{XIC}_{\text{Monomer}}}{\text{UV}_{\text{Dimer}}/\text{UV}_{\text{Monomer}}} \quad (1)$$

where $\text{XIC}_{\text{Dimer}}$ and $\text{XIC}_{\text{Monomer}}$ represent the integrated XIC peak areas of the monomer signal appearing in the dimer elution and monomer elution regions, respectively; UV_{Dimer} and $\text{UV}_{\text{Monomer}}$ represent the integrated UV peak areas of the dimer and monomer peaks, respectively. In this calculation, the noncovalent dimer is quantified using the PCD-induced monomer signal in the dimer elution region and normalized against the real monomer signal. As only the monomer signal was used, discrepancy in MS responses of different species (e.g., dimer vs monomer) can be mitigated, leading to more reliable quantitation. Using this strategy, the relative abundances of the noncovalent dimer within the total HMW species were estimated at ~11% and ~86% in lot 1 and lot 2 DS samples, respectively. Additionally, the nondissociable dimers in lot 1 and lot 2 samples also exhibited different elution profiles, where lot 2 showed a higher level of the early eluting species. (Figure 5a, blue trace). Consistently, further analysis of the dimer interactions at the subdomain level (e.g., after IdeS digestion) (Figure 5b) also revealed higher levels of noncovalent complexes in lot 2 DS sample, including the noncovalent F(ab)′$_2$ dimer (Figure 5b, magenta trace, represented by XIC of dissociated F(ab)′$_2$ monomer) and the noncovalent Fc dimer (Figure 5b, brown trace, represented by XIC of dissociated Fc/2 monomer). The nondissociable complexes including the nondissociable F(ab)′$_2$ dimer (Figure 5b, blue trace, represented by XIC of nondissociated F(ab)′$_2$ dimer) and the nondissociable F(ab)′$_2$-Fc heterodimer (Figure 5b, orange trace, represented by XIC of nondissociated F(ab)′$_2$-Fc dimer) were also detected in both lots. In particular, the nondissociable F(ab)′$_2$ dimer displayed a similar elution profile (Figure 5b, blue trace) as observed at the intact level (Figure 5a, blue trace), showing two partially separated peaks in both lots. Consistently, compared to lot 1, lot 2 showed a much higher level of the early eluting, nondissociable F(ab)′$_2$ dimer species (Figure 5a,b, blue trace). Subsequently, accurate mass measurement of the nondissociable complexes was achieved by removing the interference from the noncovalent complexes under PCD conditions and was then used to study the nature of interactions. Compared to the observed mass of a noncovalent F(ab)′$_2$ dimer (e.g., formed via gas phase association of monomer species at monomer elution time), the late-eluting, nondissociable F(ab)′$_2$ dimer consistently exhibited a mass decrease of approximately 15−19 Da, suggesting the potential presence of a covalent cross-link with a negative delta mass. In contrast, the observed mass of the early eluting, nondissociable F(ab)′$_2$ dimer was comparable to that of a noncovalent dimer, suggesting they were formed either via a small covalent cross-link or through a strong noncovalent interaction that was maintained under PCD conditions (Table S3). Lastly, the nondissociable F(ab)′$_2$−Fc heterodimers in both lot 1 and lot 2 exhibited a broad elution profile (Figure 5b, orange trace), which was attributed to three different species including (1) a [F(ab)′$_2$-Fc]+14 Da covalent dimer likely formed via a His−His cross-link; (2) a [F(ab)′$_2$-Fc] covalent dimer with an unknown cross-link with a negative delta mass of ~30 Da; and (3) a [F(ab)′$_2$-Fc]-18 Da complex due to incomplete IdeS digestion (Fc/2-clipped mAb) (Table S3). Together, the differences in HMW profile between the two DS lots as a result of process changes can be examined in great detail and attributed to differences at subdomain level interactions. Although a complete understanding of these interactions (the exact covalent cross-links in particular) might still require offline fractionation and further characterization, the rapid analysis of the unfractionated DS samples provided the necessary information to assess the impact from process changes and to build a framework for risk assessment.

PCD-Assisted nSEC-MS Analysis of Hetero-Intermolecular Interactions in Coformulated mAb Samples. Characterization of the HMW species formed in coformulated mAb drug product (DP) samples (e.g., containing more than one therapeutic mAbs) under storage or stability conditions is important over the course of development.[32] Such analysis, however, presents unique analytical challenges due to the highly complex HMW profiles frequently present in these samples involving both the homo- and hetero-intermolecular interactions.[33] To tackle these challenges, the utility of the PCD-assisted nSEC-MS method was also evaluated in studies to support the development of coformulated mAb programs. As an example, a coformulated DP sample consisting of two mAbs (mAb-A and mAb-B) were tested under accelerated stability conditions. Three major HMW species, namely, mAb-A homodimer, mAb-B homodimer, and mAb-A/B heterodimer, were readily identified in both T0 (unstressed, total HMW% = 0.7%) and T6m (25 °C for 6 months, total HMW%

https://doi.org/10.1021/jasms.1c00289
J. Am. Soc. Mass Spectrom. 2021, 32, 2885−2894

= 1.5%) samples by nSEC-MS analysis based on their different molecular weights (Figure 6, Figure S1). Using the integrated

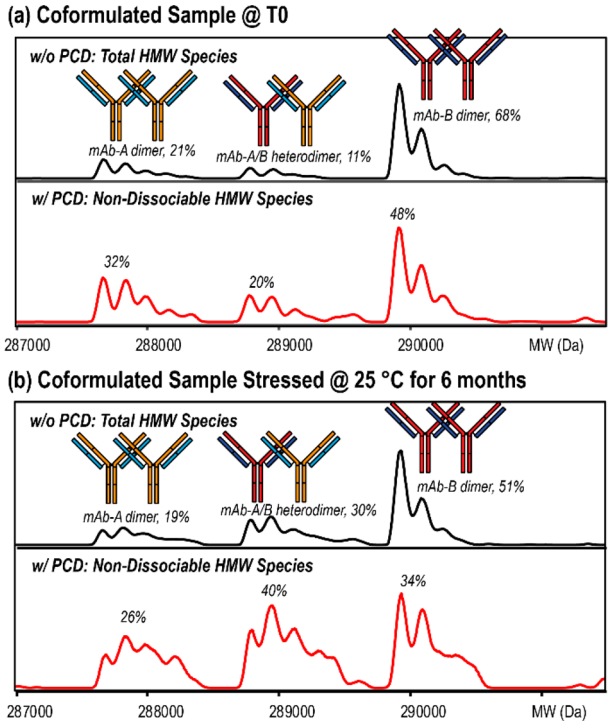

Figure 6. HMW species detected in coformulated mAb-A and mAb-B samples at (a) T0 and (b) 25 °C for 6 months using nSEC-MS under both native (black trace) and PCD (red trace) conditions. The relative abundance of each dimer was estimated using the integrated peak areas from the deconvoluted mass spectra and annotated.

peak areas from the deconvoluted mass spectra, the relative abundances of the three dimers could be estimated. Interestingly, in addition to the two homodimers a low but noticeable level of the mAb-A/B heterodimer was readily detected in the T0 sample (Figure 6a), suggesting the hetero-intermolecular interaction was likely initiated spontaneously when the two mAbs were mixed. After being stored at 25 °C for 6 months, the relative abundance of the mAb-A/B heterodimer increased significantly (from 11% to 30%), while the abundances of the mAb-A homodimer and the mAb-B homodimer remained unchanged or decreased, respectively. This observation suggested that the mAb-A/B heterodimer grew at a faster rate than the homodimers under the accelerated stability conditions. In addition, with the application of PCD the same calculation and comparison can be made for the nondissociable dimer species (Figure 6, red trace), providing a high-level assessment of the interaction nature. For example, under PCD conditions a notable decrease in relative abundance was observed for the mAb-B homodimer in both T0 and T6m samples, suggesting the noncovalent interaction contributed more significantly to the formation of mAb-B homodimer than the other two species (i.e., mAb-A homodimer and mAb-A/B heterodimer). Consistent with this observation, the dissociated mAb-B monomer also showed a much higher abundance than that of the dissociated mAb-A monomer (Figure S2), suggesting the higher dissociation rate of mAb-B homodimers than mAb-A homodimer or mAb-A/B heterodimer. In addition, it was observed that the non-dissociable mAb-A/B heterodimer exhibited a faster growth rate (from 20% to 40%) and became the most abundant nondissociable dimer species after 6 months. This rapid analysis showed that the hetero-intermolecular interaction between mAb-A and mAb-B was favorable under accelerated stability conditions, likely via covalent cross-links or tight but noncovalent interactions. This information was valuable to guide the future investigation to elucidate the exact interactions responsible for the heterodimerization, and therefore, facilitate the formulation development to minimize this type of interaction.

CONCLUSION

Comprehensive characterization of the HMW size variants is highly important during the development of therapeutic mAbs. In this study, we reported the development of a PCD-assisted nSEC-MS method that enables efficient dissociation of the noncovalent HMW complexes for improved MS characterization. Specifically, application of PCD not only allows differential detection but also improves identification of both noncovalent and nondissociable HMW species. By confirming the constituent subunits, the identification of large and unexpected noncovalent HMW complexes can be achieved with greater confidence. By removing the interference from the coeluting, noncovalent species, more accurate mass measurement of the nondissociable HMW complexes can be obtained, and therefore, facilitate the identification of the potential cross-links. Furthermore, using this method, the elution profile of each HMW complex can be readily reconstructed using XICs of either the intact ensemble (for nondissociable species) or the constituent subunits (for noncovalent species), which adds further confidence to the identification. Because of the excellent sensitivity and specificity, this method is highly effective in elucidating the complex HMW species directly from the unfractionated DS samples, making it ideally suited for tasks requiring fast turn-around. Furthermore, the utility of this method was demonstrated in different applications, including in-depth HMW characterization at late stage development, comparability assessments, and for forced degradation studies. Finally, with the growing complexity of mAb therapeutic formats (e.g., bsAb and coformulation), this method is a valuable addition to our analytical arsenal to take on the increasing challenges associated with HMW variants characterization.

ASSOCIATED CONTENT

Supporting Information

The Supporting Information is available free of charge at https://pubs.acs.org/doi/10.1021/jasms.1c00289.

Native SEC-UV traces of coformulated mAb-A and mAb-B; mass spectrum of dissociated mAb-A and mAb-B monomers from PCD-assisted nSEC-MS analysis of dimers in coformulated mAb-A and mAb-B DP sample (25 °C 6 months); summary of size variant masses associated with FabRICATOR-digested and deglycosylated enriched mAb3 HMW sample; summary of size variant masses associated with deglycosylated bsAb sample; summary of nondissociable dimeric species detected in mAb4 lot 1 and lot 2 DS samples (PDF)

https://doi.org/10.1021/jasms.1c00289
J. Am. Soc. Mass Spectrom. 2021, 32, 2885−2894

AUTHOR INFORMATION

Corresponding Authors

Shunhai Wang − *Analytical Chemistry Group, Regeneron Pharmaceuticals Inc., Tarrytown, New York 10591-6707, United States;* orcid.org/0000-0003-4055-2187; Email: shunhai.wang@regeneron.com

Yuetian Yan − *Analytical Chemistry Group, Regeneron Pharmaceuticals Inc., Tarrytown, New York 10591-6707, United States*; Email: yuetian.yan@regeneron.com

Authors

Tao Xing − *Analytical Chemistry Group, Regeneron Pharmaceuticals Inc., Tarrytown, New York 10591-6707, United States*

Anita P. Liu − *Analytical Chemistry Group, Regeneron Pharmaceuticals Inc., Tarrytown, New York 10591-6707, United States*

Zhengqi Zhang − *Analytical Chemistry Group, Regeneron Pharmaceuticals Inc., Tarrytown, New York 10591-6707, United States*

Ning Li − *Analytical Chemistry Group, Regeneron Pharmaceuticals Inc., Tarrytown, New York 10591-6707, United States*

Complete contact information is available at: https://pubs.acs.org/10.1021/jasms.1c00289

Notes

The authors declare the following competing financial interest(s): Y.Y., T.X., A.P.L., Z.Z., S.W., and N.L. are full-time employees and shareholders of Regeneron Pharmaceuticals Inc.

ACKNOWLEDGMENTS

This study was sponsored by Regeneron Pharmaceuticals Inc. The authors would like to thank Ashley Roberts of the Scientific Writing Group for their assistance in drafting and editing the manuscript.

REFERENCES

(1) Roberts, C. J. Therapeutic protein aggregation: mechanisms, design, and control. *Trends Biotechnol.* **2014**, *32* (7), 372−380.

(2) Cordoba, A. J.; Shyong, B. J.; Breen, D.; Harris, R. J. Non-enzymatic hinge region fragmentation of antibodies in solution. *J. Chromatogr. B: Anal. Technol. Biomed. Life Sci.* **2005**, *818* (2), 115−121.

(3) Xiang, T.; Lundell, E.; Sun, Z.; Liu, H. Structural effect of a recombinant monoclonal antibody on hinge region peptide bond hydrolysis. *J. Chromatogr. B: Anal. Technol. Biomed. Life Sci.* **2007**, *858* (1−2), 254−262.

(4) Wang, S.; Liu, A. P.; Yan, Y.; Daly, T. J.; Li, N. Characterization of product-related low molecular weight impurities in therapeutic monoclonal antibodies using hydrophilic interaction chromatography coupled with mass spectrometry. *J. Pharm. Biomed. Anal.* **2018**, *154*, 468−475.

(5) Vlasak, J.; Ionescu, R. Fragmentation of monoclonal antibodies. *MAbs* **2011**, *3* (3), 253−263.

(6) Paul, R.; Graff-Meyer, A.; Stahlberg, H.; Lauer, M. E.; Rufer, A. C.; Beck, H.; Briguet, A.; Schnaible, V.; Buckel, T.; Boeckle, S. Structure and function of purified monoclonal antibody dimers induced by different stress conditions. *Pharm. Res.* **2012**, *29* (8), 2047−2059.

(7) Narhi, L. O.; Schmit, J.; Bechtold-Peters, K.; Sharma, D. Classification of protein aggregates. *J. Pharm. Sci.* **2012**, *101* (2), 493−498.

(8) Parenky, A.; Myler, H.; Amaravadi, L.; Bechtold-Peters, K.; Rosenberg, A.; Kirshner, S.; Quarmby, V. New FDA draft guidance on immunogenicity. *AAPS J.* **2014**, *16* (3), 499−503.

(9) Lebowitz, J.; Lewis, M. S.; Schuck, P. Modern analytical ultracentrifugation in protein science: a tutorial review. *Protein Sci.* **2002**, *11* (9), 2067−2079.

(10) Hughes, H.; Morgan, C.; Brunyak, E.; Barranco, K.; Cohen, E.; Edmunds, T.; Lee, K. A multi-tiered analytical approach for the analysis and quantitation of high-molecular-weight aggregates in a recombinant therapeutic glycoprotein. *AAPS J.* **2009**, *11* (2), 335−341.

(11) Lowe, D.; Dudgeon, K.; Rouet, R.; Schofield, P.; Jermutus, L.; Christ, D. Aggregation, stability, and formulation of human antibody therapeutics. *Adv. Protein Chem. Struct. Biol.* **2011**, *84*, 41−61.

(12) Zolls, S.; Tantipolphan, R.; Wiggenhorn, M.; Winter, G.; Jiskoot, W.; Friess, W.; Hawe, A. Particles in therapeutic protein formulations, Part 1: overview of analytical methods. *J. Pharm. Sci.* **2012**, *101* (3), 914−935.

(13) Rouby, G.; Tran, N. T.; Leblanc, Y.; Taverna, M.; Bihoreau, N. Investigation of monoclonal antibody dimers in a final formulated drug by separation techniques coupled to native mass spectrometry. *MAbs* **2020**, *12* (1), 1781743.

(14) Lu, C.; Liu, D.; Liu, H.; Motchnik, P. Characterization of monoclonal antibody size variants containing extra light chains. *MAbs* **2013**, *5* (1), 102−113.

(15) Remmele, R. L., Jr.; Callahan, W. J.; Krishnan, S.; Zhou, L.; Bondarenko, P. V.; Nichols, A. C.; Kleemann, G. R.; Pipes, G. D.; Park, S.; Fodor, S.; Kras, E.; Brems, D. N. Active dimer of Epratuzumab provides insight into the complex nature of an antibody aggregate. *J. Pharm. Sci.* **2006**, *95* (1), 126−145.

(16) Iwura, T.; Fukuda, J.; Yamazaki, K.; Kanamaru, S.; Arisaka, F. Intermolecular interactions and conformation of antibody dimers present in IgG1 biopharmaceuticals. *J. Biochem.* **2014**, *155* (1), 63−71.

(17) Plath, F.; Ringler, P.; Graff-Meyer, A.; Stahlberg, H.; Lauer, M. E.; Rufer, A. C.; Graewert, M. A.; Svergun, D.; Gellermann, G.; Finkler, C.; Stracke, J. O.; Koulov, A.; Schnaible, V. Characterization of mAb dimers reveals predominant dimer forms common in therapeutic mAbs. *MAbs* **2016**, *8* (5), 928−940.

(18) Iacob, R. E.; Bou-Assaf, G. M.; Makowski, L.; Engen, J. R.; Berkowitz, S. A.; Houde, D. Investigating monoclonal antibody aggregation using a combination of H/DX-MS and other biophysical measurements. *J. Pharm. Sci.* **2013**, *102* (12), 4315−4329.

(19) Zhang, A.; Singh, S. K.; Shirts, M. R.; Kumar, S.; Fernandez, E. J. Distinct aggregation mechanisms of monoclonal antibody under thermal and freeze-thaw stresses revealed by hydrogen exchange. *Pharm. Res.* **2012**, *29* (1), 236−250.

(20) Yan, Y.; Wei, H.; Jusuf, S.; Krystek, S. R., Jr.; Chen, J.; Chen, G.; Ludwig, R. T.; Tao, L.; Das, T. K. Mapping the Binding Interface in a Noncovalent Size Variant of a Monoclonal Antibody Using Native Mass Spectrometry, Hydrogen-Deuterium Exchange Mass Spectrometry, and Computational Analysis. *J. Pharm. Sci.* **2017**, *106* (11), 3222−3229.

(21) Deperalta, G.; Alvarez, M.; Bechtel, C.; Dong, K.; McDonald, R.; Ling, V. Structural analysis of a therapeutic monoclonal antibody dimer by hydroxyl radical footprinting. *MAbs* **2013**, *5* (1), 86−101.

(22) Lazar, A. C.; Wang, L.; Blattler, W. A.; Amphlett, G.; Lambert, J. M.; Zhang, W. Analysis of the composition of immunoconjugates using size-exclusion chromatography coupled to mass spectrometry. *Rapid Commun. Mass Spectrom.* **2005**, *19* (13), 1806−1814.

(23) Muneeruddin, K.; Thomas, J. J.; Salinas, P. A.; Kaltashov, I. A. Characterization of small protein aggregates and oligomers using size exclusion chromatography with online detection by native electrospray ionization mass spectrometry. *Anal. Chem.* **2014**, *86* (21), 10692−10699.

(24) Ehkirch, A.; Hernandez-Alba, O.; Colas, O.; Beck, A.; Guillarme, D.; Cianferani, S. Hyphenation of size exclusion chromatography to native ion mobility mass spectrometry for the analytical characterization of therapeutic antibodies and related

products. *J. Chromatogr. B: Anal. Technol. Biomed. Life Sci.* **2018**, *1086*, 176−183.
(25) Haberger, M.; Leiss, M.; Heidenreich, A. K.; Pester, O.; Hafenmair, G.; Hook, M.; Bonnington, L.; Wegele, H.; Haindl, M.; Reusch, D.; Bulau, P. Rapid characterization of biotherapeutic proteins by size-exclusion chromatography coupled to native mass spectrometry. *MAbs* **2016**, *8* (2), 331−339.
(26) Yan, Y.; Xing, T.; Wang, S.; Li, N. Versatile, Sensitive, and Robust Native LC-MS Platform for Intact Mass Analysis of Protein Drugs. *J. Am. Soc. Mass Spectrom.* **2020**, *31* (10), 2171−2179.
(27) Rose, R. J.; Labrijn, A. F.; van den Bremer, E. T.; Loverix, S.; Lasters, I.; van Berkel, P. H.; van de Winkel, J. G.; Schuurman, J.; Parren, P. W.; Heck, A. J. Quantitative analysis of the interaction strength and dynamics of human IgG4 half molecules by native mass spectrometry. *Structure* **2011**, *19* (9), 1274−1282.
(28) Kaltashov, I. A.; Mohimen, A. Estimates of protein surface areas in solution by electrospray ionization mass spectrometry. *Anal. Chem.* **2005**, *77* (16), 5370−5379.
(29) Xu, C. F.; Chen, Y.; Yi, L.; Brantley, T.; Stanley, B.; Sosic, Z.; Zang, L. Discovery and Characterization of Histidine Oxidation Initiated Cross-links in an IgG1Monoclonal Antibody. *Anal. Chem.* **2017**, *89* (15), 7915−7923.
(30) Powell, T.; Knight, M. J.; Wood, A.; O'Hara, J.; Burkitt, W. Photoinduced cross-linking of formulation buffer amino acids to monoclonal antibodies. *Eur. J. Pharm. Biopharm.* **2021**, *160*, 35−41.
(31) Liu, M.; Zhang, Z.; Cheetham, J.; Ren, D.; Zhou, Z. S. Discovery and characterization of a photo-oxidative histidine-histidine cross-link in IgG1 antibody utilizing (1)(8)O-labeling and mass spectrometry. *Anal. Chem.* **2014**, *86* (10), 4940−4948.
(32) *Guidance for industry: codevelopment of two or more new investigational drugs for use in combination.. Center for drug evaluation and research*; U.S. Food and Drug Administration: Rockville, MD, 2013.
(33) Kim, J.; Kim, Y. J.; Cao, M.; De Mel, N.; Albarghouthi, M.; Miller, K.; Bee, J. S.; Wang, J.; Wang, X. Analytical characterization of coformulated antibodies as combination therapy. *MAbs* **2020**, *12* (1), 1738691.

https://doi.org/10.1021/jasms.1c00289
J. Am. Soc. Mass Spectrom. 2021, 32, 2885−2894